Effects of Intra-Articular D-Amino Acids Combined With Systemic Vancomycin on an Experimental *Staphylococcus Aureus*-Induced Periprosthetic Joint Infection

Yicheng Li
Department of Orthopaedics, First Affiliated Hospital of Xinjiang Medical University, Urumqi
Shalitanati Wuermanbieke
Karamay Central Hospital of Xinjiang
Jiangdong Ren
Department of Orthopaedics, First Affiliated Hospital of Xinjiang Medical University, Urumqi
Wenbo Mu
Department of Orthopaedics, First Affiliated Hospital of Xinjiang Medical University, Urumqi
Hairong Ma
State Key Laboratory of Pathogenesis, Prevention and Treatment of High Incidence Diseases in Central Asian Xinjiang Key Laboratory of Echinococcosis, Clinical Medical Research Institute
Fei Qi
Department of Orthopaedics, First Affiliated Hospital of Xinjiang Medical University, Urumqi
Xiaoyue Sun
Department of Orthopaedics, First Affiliated Hospital of Xinjiang Medical University, Urumqi
Yang Liu
Department of Orthopaedics, First Affiliated Hospital of Xinjiang Medical University, Urumqi
Abdusami Amat
Department of Orthopaedics, First Affiliated Hospital of Xinjiang Medical University, Urumqi
Xiaogang Zhang
Department of Orthopaedics, First Affiliated Hospital of Xinjiang Medical University, Urumqi
Li Cao (xjbone@sina.com)
Department of Orthopaedics, First Affiliated Hospital of Xinjiang Medical University, Urumqi

---

Research Article

Keywords: PJI, arthroplasty, vancomycin, periprosthetic

Posted Date: December 3rd, 2020

DOI: https://doi.org/10.21203/rs.3.rs-113375/v1

Version of Record: A version of this preprint was published at Journal of Microbiology, Immunology and Infection on February 1st, 2022. See the published version at https://doi.org/10.1016/j.jmii.2022.01.005.

Abstract

Periprosthetic joint infection (PJI) after joint arthroplasty remains a devastating complication in which the formation of a bacterial biofilm is the major cause of treatment failure. The D-isoforms of amino acids (D-AAs) exhibit anti-biofilm potential against a diverse range of bacterial species *in vitro*, while its role *in vivo* remains unclear. The aim of this study was to investigate the effects of a combination of D-AAs and vancomycin on a PJI rat model. Eight-week-old male SD rats were randomized to the control group, sham group, vancomycin group, D-AAs-vancomycin group. After treatment for 6 weeks, the group treated with a D-AAs-vancomycin combination sustained normal weight gain and exhibited reduced the serum levels of α2M, IL-1β, IL-6, IL-10, TNF-α and PGE2. Moreover, treated with D-AAs in combination with vancomycin improved the weight-bearing activity performance, increased the sizes and widths of distal femurs, and improved Rissing scale scoring. In particular, treatment using D-AAs enhanced the ability of vancomycin to eradicate *Staphylococcus aureus*, as demonstrated by the dispersion of existing biofilms and the inhibition of biofilm formation that occurred in a concentration-dependent manner. This treatment combination also resulted in a reduction in bacterial burden with in the soft tissues, bones, and implants. Furthermore, D-AAs-vancomycin combination treatment attenuated abnormal bone remodelling around the implant, as evidenced by an observed increase in MBD, BV/TV, and Tb.Th and the presence of reduced Trap+ osteoclasts and elevated osterix+ osteo-progenitors. In conclusion, combining D-AAs with vancomycin provides an effective therapeutic strategy for the treatment of PJI by promoting biofilm dispersion to enhance antimicrobial activity.

Introduction

Periprosthetic joint infection (PJI) represents one of the most devastating complications that can occur following joint replacement surgery. Although the rates of PJI after primary arthroplasty have remained between 1% and 3%, recent analyses predict that the incidence of PJI will reach up to 4 million cases per year in the United States by 2030[1]. The increasing prevalence of PJI will result in a projected financial burden for PJI in excess of $1.6 billion by 2020[1]. Despite recent advances in antiseptic protocols[2], surgical techniques[3] and operating-room sterility[4], efforts to prevent and treat PJI remain challenging.

Compared to other complications that can arise after joint replacement, PJI is difficult to treat due to the formation of a microbial biofilm that occurs as an adaptive response to hostile environments to protect the invading bacteria against the immune system and complement system of the host[5,6]. Specifically, the biofilm augments bacterial resistance against the routine antibiotics by approximately 1000-fold[7] by impairing the penetration of antibiotics through the extracellular constituents[8] and by decreasing the metabolic activity of biofilm-embedded microorganisms[9]. Additionally biofilms promote the presence of slow-growing or quiescent “persister cells”[10,11]. Consequently, the higher values of minimum biofilm inhibitory concentration (MBIC) for the bacteria result in inadequate antibiotic treatment[12], which can promote the appearance of mutated antibiotic-resistant strains[13]. Additionally, bacterial enterotoxins and the activation of polymorphonuclear neutrophils can elicit active bone resorption and inhibit bone

formation, ultimately resulting in loosening of the prosthesis[14]. Therefore, there is an urgent need to develop strategies to disrupt the dense biofilm microarchitecture so as to promote the antibiotis flux towards deeper cell layers to kill bacteria within the biofilm.

The D-isoforms of amino acids (D-AAs) have been proved to break down biofilms in a diverse range of bacterial species, including *Bacillus subtilis* and *Staphylococcus aureus*[15]. In contrast to chemical agents used to disperse biofilms, D-AAs exhibit minimal cellular toxicity and can disturb the initial attachment of the bacteria to the surface while inhibiting subsequent growth of the microcolony into larger bacterial communities[16]. Moreover, the anti-biofilm activities of D-AAs are associated with multiple mechanisms, including the reduction of gene expression that is involved in extracellular matrix production[17] and the diminishment of the surface expression of fibers that are required for biofilm formation that results from the incorporation of D-AAs into the bacterial cell wall[18]. However, it remains unclear if D-AAs are capable of disassembling biofilms and promoting antibacterial activity in the context of PJI.

Based on these previous findings, we hypothesised that combining dispersal agents with antibiotics may provide an effective therapeutic strategy for PJI by functionally enhancing antimicrobial activity via the biofilm dispersion. To investigate this hypothesis, we assessed the efficacy of a combination therapy of D-AAs with vancomycin against a rat model of a *Staphylococcus aureus*-induced PJI.

Results

Effects of D-AAs-vancomycin combination therapy on systemic and local responses *in vivo.*

There were no signs of systemic illness in the rats that survived the postoperative period. For systemic response, a reduction in body weight was induced in the sham group at postoperative 8 weeks relative to that of the control group and vancomycin plus D-AAs group; however, there was no significant difference between the control group and vancomycin plus D-AAs group (Fig. 2A). Moreover, the sham group exhibited a prominent increase in the levels of α2M, IL-1β, IL-6, IL-10, TNF-α and PGE2 compared to those of the control group, while PJI rats treated with vancomycin plus D-AAs but not vancomycin alone exhibited no statistical difference in these factors compared to these factors in the controls (Fig. 2B-G).

For local response, our findings revealed that weight-bearing activity was markedly decreased following PJI and PJI rats treated with vancomycin alone, while the combination of D-AAs and vancomycin improved weight-bearing activity to a level similar to that of the controls (Fig. 3A,B). Moreover, rats provided with sham treatment, the sizes and widths of distal femurs were obviously reduced in rats treated with vancomycin or a D-AAs-vancomycin combination, and no statistically significant difference was observed between the D-AAs plus vancomycin and control groups (Fig. 4A-C). Additionally, D-AAs-vancomycin combination therapy clearly reduced the Rissing scale score of PJI rats to levels that were similar to those of the controls (Fig. 3C). Taken together, D-AAs-vancomycin combination therapy was more effective than was vancomycin alone in inhibiting infection-induced systemic and local responses.

Effects of D-AAs on biofilm formation*in vivo* and *in vitro.*

Scanning electron microscopy (SEM) was performed to confirm the efficacy of biofilm dispersion in response to D-AAs in rat PJI models. In the formal experiment, substantial biofilm formation and large clusters of cocci were visualised around the surface of the implant in the sham and vancomycin groups, while the D-AAs plus vancomycin group did not possess detectable levels of dense biofilm or even colonised bacteria, and this finding was similar to that from the control group (Fig. 5A). Moreover, D-AAs exhibited the capacity to dissociate biofilms in a dose-dependent manner; however, D-AAs failed to clear the colonised bacteria (Fig. 5B).

Subsequently, the activity of D-AAs in regard to biofilm disassembly and prevention was further determined *in vitro* using crystal violet staining. D-Trp, D-Pro, and D-Phe dispersed biofilms in a dose-dependent manner and were most effective at concentrations of 10 mM (Fig. 6A,B). Additionally, D-Trp, D-Pro, and D-Phe prominently inhibited biofilm formation when *Staphylococcus aureus* was cultured in the presence of individual D-AAs (Fig. 6C). Importantly, the biofilm-dispersive activity of the mixture of D-AAs was elevated, and a reduction in biofilm biomass was observed at a concentration of 1 mM (Fig. 6B,C). In parallel, individual D-AAs at a concentration of 10 mM exhibited the ability to dissociate existing biofilms and to prevent biofilm formation by the clinical strains (Fig. 6D,E). Collectively, D-AAs possess the potential for anti-biofilm activity *in vivo* and *in vitro*.

Effects of D-AAs on the antibacterial activity of vancomycin*in vivo* and *ex vivo.*

To determine if biofilm disassembly by D-AAs promotes the ability of vancomycin to clear bacteria, CFUs were isolated from peri-implant bone, soft tissue, and implants. The CFUs for the tissue specimens were statistically higher in the sham group compared to those in the groups treated with vancomycin alone or a D-AAs-vancomycin combination (Fig. 7A,B). The implants in the sham group also exhibited significantly higher CFUs compared to those of the combined treatment group; however there were no differences in comparison to the group treated with vancomycin alone (Fig. 7C).

Next, we further assessed the efficacy of D-AAs-vancomycin combined therapy versus vancomycin alone in clearing the infection. The results demonstrated that a markedly higher proportion of soft tissue, bone, and implant cultures was positive in the sham group (soft tissue: 100% [8 of 8], bone: 100% [8 of 8], implant: 100% [8 of 8]) compared to these values in the groups treated with vancomycin alone (implant: 38% [3 of 8]) or with a D-AAs-vancomycin combination (soft tissue: 13% [1 of 8], bone: 25% [2 of 8], implant: 0% [0 of 8]). Additionally, the proportions of positive cultures in the groups treated with vancomycin alone (soft tissue: 50%; bone: 75%) were not significantly different from those in the sham group (Fig. 7D,E). Importantly, the D-AAs-vancomycin combination therapy was superior to therapy using vancomycin alone in regard to the proportions of positive cultures in the bone and to implant analyses (Fig. 7E,F). Of note, there was no significant difference between the D-AAs-vancomycin combination-treated group and the control group (Fig. 7D-F).

Effects of D-AAs-vancomycin combination therapy on aberrant bone remodelling *in vivo.*

Finally, μCT analyses and staining were applied to assess the changes in the microstructure and bone remodelling of the distal femur. The findings revealed that vancomycin alone and the D-AAs-vancomycin combination treatment resulted in higher MBD, BV/TV, and Tb.Th values than those observed in sham-treated rats (Fig. 8A-E). Moreover, no significant difference was noted between the D-AAs-vancomycin-treated rats and the uninfected controls (Fig. 8A-E). Additionally, the number of $Trap^+$ osteoclasts in the sham group was markedly reduced in the D-AAs plus vancomycin group (Fig. 9A,C). Minimal levels of $osterix^+$ cells were observed in infected rats, while the D-AAs-vancomycin combination restored $osterix^+$ cells to levels similar to those of uninfected rats (Fig. 9B,D). Notably, the number of $osterix^+$ cells failed to recover in response to treatment with vancomycin alone. Collectively, abnormal bone remodelling around the prosthesis was prominently attenuated by biofilm disruption and bacterial elimination.

Discussion

This study was the first to assess the efficacy of a D-AAs-vancomycin combination therapy using a rat PJI model. As expected, although systemic vancomycin improved systemic and local responses and decreased bacterial burden, this therapy failed to eliminate the infection in all cases. However, the combination treatment of D-AAs and vancomycin achieved a marked therapeutic benefit relative to that of vancomycin alone. Mechanistically, D-AAs prevented biofilm formation and disassembled established biofilms, thus facilitating the diffusion of vancomycin into the deeper cell layers to eradicate bacteria. Additionally, we also found that the D-AAs-vancomycin combination therapy was highly effective at redressing abnormal bone remodelling by re-establishing the dynamic balance between bone resorption and formation.

Despite meticulous clinical management that incorporates irrigation, surgical debridement, and the use of antibiotics[19], a small percentage of “persister cells” in biofilms can still survive and rapidly grow after the cessation of antimicrobial therapy, thus leading to recurrent PJIs[20]. Therefore, dissociation of these biofilms may provide a vital target for PJI therapy. Recent studies have shown considerable interest in biofilm dispersal agents such as D-AAs[21], quorum-sensing inhibitors[22], and vapour nanobubbles[23]. A previous study demonstrated the efficacy of the local delivery of D-AAs in eliminating bacterial contamination by targeting bacteria within biofilms[24]. Similarly, a rat model in our study strictly mimicked clinical PJI, where mature biofilm formation occurred 2 weeks after bacterial colonisation on the prosthesis surface[25]. Notably, a mixture of D-AAs that included D-Trp, D-Pro, and D-Phe was active in not only dispersing mature biofilms but also in inhibiting biofilm formation to expose colonised bacteria to vancomycin to achieve a stronger sterilisation effect. Moreover, our *in vitro* findings also confirmed that the concentrations of ≥ 1 mM of D-Trp, D-Pro and D-Phe prevent biofilm formation and disrupt the existing biofilm integrity of *Staphylococcus aureus.* Specifically, the identified concentrations exhibited the effects of biofilm-dispersive and anti-biofilm activity against various clinical strains. However, strain heterogeneity and different bacterial species result in a discrepancy in regard to anti-biofilm activity. Hochbaum *et al*. found that the dispersive activity of D-Tyr, D-Pro, and D-Phe on biofilms produced by the *Staphylococcus aureus* WT strain could be observed at concentrations as low as 500 μM[26]. Sanchez *et*

al. revealed the effect of D-Met, D-Pro, and D-Trp on biofilm disruption at concentrations of ≥ 5 mM[27]. Despite existing differences in individual interventions, our study is consistent with the previous studies[26,27] that demonstrated that an equimolar mixture of D-AAs shifted the dose-response curve toward lower doses compared to that of the individual D-AAs. Collectively, the anti-biofilm activity of D-AAs highlights their potential usefulness in the treatment of PJI.

The cell wall thickness of *S. aureus* located in biofilms gradually increases[25], thereby resulting in reduced susceptibility to vancomycin[28]. In this case, the effect of vancomycin on inhibiting bacterial cell wall synthesis was significantly reduced[29]. In contrast, D-AAs can modulate cell wall remodelling in bacteria by causing the release of amyloid fibres that link the cells in the biofilm together[15]. Although D-AAs are unable to kill bacteria[30], they can likely provide an effective adjuvant therapy that can be used in combination with antibiotics. Indeed, our results revealed that the use of D-AAs significantly elevated the bactericidal activity of vancomycin, where 1- to 2-log CFUs decreases were observed compared to decreases caused by the agent alone. Furthermore, combining D-AAs with vancomycin therapy is more effective than vancomycin therapy is more effective than is the use of vancomycin alone in regard to the reduction of systemic and local reactions and the attenuation of X-ray results. This result was somewhat unanticipated, as the vancomycin-D-AAs combination was applied in the absence of debridement or irrigation, both of which were routinely performed in our previous clinical studies[31]. This may be attributed to the possibility that interventions using D-AAs augment the ability of drugs to diffuse into deeper cell layers by establishing more cracks between bacteria to ultimately eradicate these bacteria.

Of note, the D-AAs-vancomycin combination therapy resulted in high infection clearance, as no *Staphylococcus aureus* bacteria were present after *ex vivo* culture of 1 of 8 soft tissue samples, 2 of 8 bone samples, or in any (8 of 8) implant samples. These results can be explained in part by a new study, which demonstrated that D-AAs resensitise *Staphylococcus aureus* to antibiotics by impairing alanine transport[33] that plays a crucial role in the remodelling of the cell wall and the integrity of peptidoglycans[15,30]. Moreover, Sanchez *et al*. also demonstrated a reduction in the MBIC and viable biofilm bacteria in response to treatment with D-AAs[12]. Taken together, in addition to anti-biofilm activity, D-AAs are capable of increasing bacterial susceptibility to antibiotics.

Bacteria or their components that can induce abnormal bone remodelling are the main causes of prosthesis loosening[14]. On the one hand, osteoclastic activity can be stimulated by *S. aureus,* including protein A[33], or its secreted substances[34]. It has been observed that soluble factors produced by *S. aureus* can reduce osteoblast viability and increase cell apoptosis and these factors can inhibit bone mineralisation[35]. Taken together, these factors drive the dynamic balance of bone remodelling towards osteolysis. Our micro-CT results also showed that the MBD, BV/TV, and Tb.Th values of the distal femur were decreased in the sham group. In parallel with the results of microarchitecture analyses, our study found increased $Trap^+$ osteoclasts and reduced $osterix^+$ osteo-progenitors around the prosthesis. However, D-AAs-vancomycin combination therapy alleviated this aberrant microstructure by reducing the number of osteoclasts and osteoblasts to normal levels, thereby stabilising the joint prosthesis.

Due to the existence of biofilms, PJI patients must be administered antibiotics for long periods of time and at high doses to control infection, and this can lead to a number of risks to patient health and impose an economic burden on the healthcare system. Fortunately, our study indicated that the combination treatment of D-AAs and vancomycin represents a potentially efficacious therapy for PJIs, as the disassembly of biofilms results in an increase in antibiotic activity, ultimately improving abnormal bone remodelling, and preventing prosthesis loosening.

Materials And Methods

Animals.

Ethical statement. All procedures complied with the guidelines of the Association for Assessment and Accreditation of Laboratory Animal Care, and the protocol was approved by the Institutional Animal Care and Use Committee of First Affiliated Hospital of Xinjiang Medical University (protocol number IACUC20191011-01).

Amino acids and bacterial strain.

D-isomers of amino acids, including phenylalanine (Phe), proline (Pro) and tryptophan (Trp), were purchased from Sigma. For bacterial cultures, D-AA stocks were prepared in 0.5 M HCl at concentrations between 150 and 200 mM. There were diluted into Mueller Hinton (MHB-II) broth that was neutralised to pH 7.4, and the stocks were then stored at - 80 °C. *Staphylococcus aureus* ATCC 25923 was used for this study. Four clinical *Staphylococcus aureus* strains that were characterised according to biofilm formation were isolated from PJI patients as described in our previous study[31] (Supplementary Table 1). For all studies, the strains were cultured at 37 °C overnight in tryptic soy broth (TSB) media with agitation.

Induction and treatment of PJI in a rat model.

Eight-week-old male Sprague-Dawley (SD) rats were purchased from the Animal Centre of Xinjiang Medical University. Animal handling conditions included a humidity of 55 ± 5%, a temperature of 25 ± 2 °C, and a 12 h light/dark cycle. All rats were maintained under specific pathogen-free conditions and provided with autoclaved food and water *ad libitum*. The rats were anaesthetized using 10% hydrated chloral solution (Aladdin, 4 mL kg^{-1} body weight). The joint capsule of the right knee was opened through a medial parapatellar arthrotomy (Fig. 1A). After exposing the intercondylar notch, the femoral canal was reamed with sequentially larger needles until an orthopaedic-grade Kirschner wire (1.0 mm in diameter and 20.0 mm in length; Synthes) was exactly inserted in a retrograde fashion with 1 mm of wire protruding into the joint space (Fig. 1B-D). The arthrotomy site was sutured using with interrupted $4^{\#}$ Monocryl (Ethicon) and then injected with *Staphylococcus aureus* (1×10^4 colony-forming units [CFUs] in 10 µL saline) (Fig. 1E,F). Finally, the skin was closed. Beginning the second week afer Kirschner wire implantation, a therapeutic dose of vancomycin (110 mg/kg twice daily) (Novaplus; Hospira, Inc., Lake Forest, IL) was administered by subcutaneous injection in the vancomycin gruop. On this basis, D-AAs were injected into the articular cavity once weekly in the vancomycin plus D-AAs group.

A preliminary experiment was performed first to identify the optimal dose of D-AAs. Rats were randomly assigned to the control group, sham group, vancomycin group, and D-AAs groups at various concentrations (0.5, 1, and 10 mM; n = 8 per group). After treatment for 6 weeks, lower concentrations of D-AAs (0.5 or 1 mM) exerted minimal effects on the local response (Supplementary Fig. 1). Based on this, in the formal experiment, the rats were randomised to the control group, sham group, vancomycin group, and a 10 mM D-AAs combined with vancomycin group (n = 20 per group, where 8 rats were used for tissue homogenate, 8 rats were used for immunostaining and 4 rats were used for SEM analysis). Additionally, 16 rats were randomly assigned to the sham group and various concentrations of D-AAs groups (0.5, 1, and 10 mM) to evaluate the biofilm lysis potential of D-AAs alone after 6 weeks by SEM.

Systemic and local response analysis.

The weights of all rats were measured and recorded once every two weeks. Serum samples were collected from the left ventricle immediately after sacrifice. The serum concentrations of α2M, IL-1β, IL-6, IL-10, TNF-α, and PGE2 were determined by ELISA according to the manufacturer's instructions (CUSABIO, China). ELISA results were quantified according to absorbance at 450 nm as assed using a microplate reader (Bio-Rad, Hercules, CA, USA), and these values were normalised according to the number of cells per well.

The weight-bearing activity of rats was assessed using ink blot analysis and was graded for each rat as full (3 points), partial (2 points), toe-touch (1 point), or non-weight-bearing (0 points)[36]. The front paws of the rats were covered with dark blue ink, and the hind paws were covered with red ink.

Radiographs were assessed using Image J software. The maximal femoral width was calculated perpendicular to the anatomical axis of the distal portion of the femur. The area of the distal 25% of the femur (from the midpoint of a line extending from the intercondylar notch to its intersection with a perpendicular line that bisected the third trochanter) was also measured. The local tissue response was evaluated at the time of implant-bone harvest according to the Rissing score[37].

SEM analysis.

After acquisition, samples were fixed with 2.5% (w/v) glutaraldehyde and 0.15 M sodium cacodylate buffer for 3 h. Samples were then rinsed with 0.15 M sodium cacodylate buffer and fixed for 1h in 1% (v/v) osmium tetroxide in sodium cacodylate buffer. Samples were dehydrated with ethanol and then incubated with hexamethyldisilizane, and this was followed by drying in a desiccator overnight. Samples were sputter-coated with gold palladium and observed using a JEOL-6610 scanning electron microscope.

Biofilm formation and dispersal assays.

Biofilm formation was assessed under static conditions for 24 h in polystyrene 24-well plates (Corning, Inc., Corning, NY, USA). Briefly, after overnight incubation, the culture medium was removed and fresh medium containing either an individual D-AA or a 1:1:1 mixture of D-Trp: D-Pro: D-Phe was added at the

indicated concentrations. After incubation for 24 h, the wells were washed with phosphate buffered saline (PBS) and then stained with 0.1% (w/v) crystal violet (Sigma Aldrich, St. Louis, MI, USA) at room temperature for 15 min. Next, biofilm biomass was examined by measuring the optical density at 570 nm of the crystal violet that was solubilised in 80% (v/v) ethanol. All assays were performed in triplicate.

Ex vivo bacterial burden.

After euthanasia, the peri-implant bone and soft tissues were harvested along with the implanted K-wires. The bone and soft tissues were homogenised using a sterile tissue grinder, and this was followed by inoculation of 20 µL aliquots onto sheep-blood agar plates (Hardy Diagnostics) for 24 h at 37 °C. The K-wires were sonicated for 10 min and then vortexed for 2 min. Subsequently, 20 µL of sonicated fluid was plated and incubated as described for tissue cultures. The number of CFUs was counted after overnight incubation of the plates. Additionally, to further confirm if the bone tissues, soft tissues, or K-wires retained any bacteria, the homogenates and sonicates were cultured again for an additional 48 h at 37°C. The presence or absence of bacterial CFUs was determined by assessing for the presence or absence of CFUs after 48 h culture of the plates.

Micro-CT analysis.

A high-resolution micro-CT (µCT) was conducted using a SkyScan 1172 Scanner. The data were subsequently reconstructed (NRecon v1.6), analysed (CTAN, v1.9), and re-established for 3D model visualisation (CTVol, v2.0). The coronal view of the 1.5 cm distal femur was selected for 3D histomorphometric analysis. Around the K-wire, a 3 mm region was identified as the region of interest. Three-dimensional structural parameters, including BMD (g cm^{-3}), BV/TV, and Tb.Th (mm), were then analysed.

Histological analysis and immunostaining.

Following euthanasia, the right knee joints of rats were harvested and fixed in 4% paraformaldehyde for 24 h. Then, the knee joints were decalcified for 3 weeks and embedded in paraffin. Sagittal sections of the femur were processed for tartrate-resistant acid phosphatase (TRAP) staining and immunostaining.

For immunostaining, the sections were rehydrated and quenched with endogenous peroxidase before treatment with 0.1% trypsin for 30 min at 37 °C to retrieve the antigen. Then, 20% normal horse serum was used to block the sections to reduce non-specific staining. Sections were then incubated with primary antibodies against osterix (Abcam, 1:400, ab22552). A horseradish peroxidase streptavidin detection system (ZSGB BIO) was used to detect the immunoactivity, and this was followed by counterstaining with haematoxylin (ZSGB BIO). The number of positively stained cells was determined in a blinded manner using cellSens software (Olympus, Int, USA).

Statistical analysis.

Graphpad Prism 5.0 was used to analyse data and to draw diagrams. Significance was determined using a One-Way ANOVA for the comparison of animal systemic and local responses, radiographic findings, and μCT findings using the nonparametric Wilcoxon rank-sum test for the comparison of *ex vivo* CFUs between different treatment conditions and using the Fisher exact test for the comparison of the percentages of cultures that exhibited any bacterial growth. A p value of < 0.05 was considered significant.

Declarations

Data availability statement.

The datasets generated for this study are available upon request from the corresponding author.

Acknowledgements

This study was supported by grants from the National Natural Science Foundation of China (No.81860746) and the Xinjiang Natural Science Foundation (No. 2018D01C187).

Author contributions

YL, SW, and LC designed the research and wrote the paper. YL, SW, JR, and WM performed the experiments. FQ, XS and HM analysed the data and edited the paper. XZ and LC contributed to the materials and reagents. XZ, AA, and LC revised the paper and guided the research.

References

1. Kurtz, S.M., *et al*. Economic burden of periprosthetic joint infection in the United States. J Arthroplasty. 27, 61-65 (2012).
2. Riesgo, A.M., *et al*. Vancomycin Povidone-Iodine Protocol Improves Survivorship of Periprosthetic Joint Infection Treated With Irrigation and Debridement. J Arthroplasty. 33, 847-850 (2018).
3. Zaruta, D.A., *et al*. Indications and Guidelines for Debridement and Implant Retention for Periprosthetic Hip and Knee Infection. Curr Rev Musculoskelet Med. 11, 347-356 (2018).
4. Parvizi, J., *et al*. Environment of care: Is it time to reassess microbial contamination of the operating room air as a risk factor for surgical site infection in total joint arthroplasty? Am J Infect Control. 45, 1267-1272 (2017).
5. Shah, S.R., Kasper, F.K., and Mikos, A.G. Perspectives on the prevention and treatment of infection for orthopedic tissue engineering applications. Chinese Science Bulletin. 2013, 58(35):4342-4348 (2013).
6. Conterno, L.O., da Silva Filho, C.R. Antibiotics for treating chronic osteomyelitis in adults. Cochrane Database Syst Rev. CD004439 (2009).
7. Wu, H., *et al*. Strategies for combating bacterial biofilm infections. Int J Oral Sci. 7, 1-7 (2015).

8. Campanac, C., *et al*. Interactions between biocide cationic agents and bacterial biofilms. Antimicrob Agents Chemother. 46, 1469-1474 (2002)..
9. Sternberg, C., *et al*. Distribution of bacterial growth activity in flow-chamber biofilms. Appl Environ Microbiol. 65, 4108-4117 (1999).
10. Waters, E.M., *et al*. Convergence of Staphylococcus aureus persister and biofilm research: can biofilms be defined as communities of adherent persister cells? PLoS Pathog. 12, e1006012 (2016).
11. Koo, H., *et al*. Targeting microbial biofilms: current and prospective therapeutic strategies. Nat. Rev. Microbiol. 15, 740-755 (2017).
12. Sanchez, C.J. Jr., *et al*. D-amino acids enhance the activity of antimicrobials against biofilms of clinical wound isolates of Staphylococcus aureus and Pseudomonas aeruginosa. Antimicrob Agents Chemother. 55, 4589-4593 (2014).
13. Gardete, S., Tomasz, A. Mechanisms of vancomycin resistance in Staphylococcus aureus. J Clin Invest. 124, 2836-2840 (2014).
14. Josse, J., *et al*. Interaction Between Staphylococcal Biofilm and Bone: How Does the Presence of Biofilm Promote Prosthesis Loosening? Front Microbiol. 10, 1602 (2019).
15. Kolodkin-Gal, I., *et al*. D-Amino Acids Trigger Biofilm Disassembly. Science. 328, 627-629 (2010).
16. Xing, S.F., *et al*. D-Amino acids inhibit initial bacterial Adhesion: Thermodynamic evidence. Biotechnol Bioeng. 112, 696-704 (2015).
17. Leiman, S.A., *et al*. D-amino acids indirectly inhibit biofilm formation in Bacillus subtilis by interfering with protein synthesis. J Bacteriol. 195, 5391-5395 (2013).
18. Cava, F., *et al*. Emerging knowledge of regulatory roles of D-amino acids in bacteria. Cell Mol Life Sci. 68, 817-831 (2011).
19. Ottesen, C.S., *et al*. Acceptable Success Rate in Patients With Periprosthetic Knee Joint Infection Treated With Debridement, Antibiotics, and Implant Retention. J Arthroplasty. 34, 365-368 (2019).
20. Percival, S.L., *et al*. Antimicrobial tolerance and the significance of persister cells in recalcitrant chronic wound biofilms. Wound Repair Regen. 19, 1-9 (2011).
21. Aliashkevich, A., Alvarez, L., Cava, F. New Insights into the Mechanisms and Biological Roles of D-Amino Acids in Complex Eco-Systems. Front Microbiol. 9, 683 (2018).
22. Brackman, G., *et al*. Quorum sensing inhibitors increase the susceptibility of bacterial biofilms to antibiotics in vitro and in vivo. Antimicrob Agents Chemother. 55, 2655-2661 (2011).
23. Teirlinck, E., *et al*. Laser-induced vapour nanobubbles improve drug diffusion and efficiency in bacterial biofilms. Nat Commun. 9, 4518 (2018).
24. Sanchez, C.J. Jr., *et al*. Effects of local delivery of D-amino acids from biofilm-dispersive scaffolds on infection in contaminated rat segmental defects. Biomaterials. 34, 7533-7543 (2013).
25. Nishitani, K., *et al*. Quantifying the natural history of biofilm formation in vivo during the establishment of chronic implant-associated Staphylococcus aureus osteomyelitis in mice to identify critical pathogen and host factors. J Orthop Res. 33, 1311-1319 (2015).

26. Hochbaum, A.I., *et al*. Inhibitory effects of D-amino acids on Staphylococcus aureus biofilm development. J Bacteriol. 193, 5616-5622 (2011).
27. Sanchez C.J. Jr., *et al*. Biofilm formation by clinical isolates and the implications in chronic infections. BMC Infect Dis. 13, 47 (2013).
28. Williams, I., *et al*. Flow cytometry and other techniques show that Staphylococcus aureus undergoes significant physiological changes in the early stages of surface-attached culture. Microbiology, 1999, 145, 1325-1333 (1999).
29. Sakoulas, G., Moellering, R.C., Eliopoulos, G.M. Adaptation of methicillin-resistant Staphylococcus aureus in the face of vancomycin therapy. Clin. Infect. Dis. 42, S40-S50 (2006).
30. Lam, H., Oh, *et al*. D-amino acids govern stationary phase cell wall remodeling in bacteria. Science. 325, 1552-1555 (2009).
31. Ji, B., *et al*. Retention of the well-fixed implant in the single-stage exchange for chronic infected total hip arthroplasty: an average of five years of follow-up. Int Orthop. 41, 901-909 (2017).
32. Gallagher, L.A., *et al*. Impaired alanine transport or exposure to d-cycloserine increases the susceptibility of MRSA to β-lactam antibiotics. J Infect Dis. 2, 1000-1016 (2020).
33. Ren, L.R., *et al*. Staphylococcus aureus protein a induces osteoclastogenesis via the NF-κB signaling pathway. Mol Med Rep. 16, 6020-6028 (2017).
34. de Mesy Bentley, K. L., *et al*. Evidence of Staphylococcus aureus deformation, proliferation, and migration in canaliculi of live cortical bone in murine models of osteomyelitis. J Bone Miner Res.32, 985-990 (2017).
35. Josse, J., Velard, F., Gangloff, S.C. Staphylococcus aureus vs. osteoblast: relationship and consequences in osteomyelitis. Front Cell Infect Microbiol. 5, 85 (2015).
36. Carli, A.V., *et al*. Quantification of Peri-Implant Bacterial Load and in Vivo Biofilm Formation in an Innovative, Clinically Representative Mouse Model of Periprosthetic Joint Infection. J Bone Joint Surg Am. 99, e25 (2016).
37. Rissing, J.P., *et al*. Model of experimental chronic osteomyelitis in rats. Infection and Immunity. 47, 581-586 (1985).

Figures

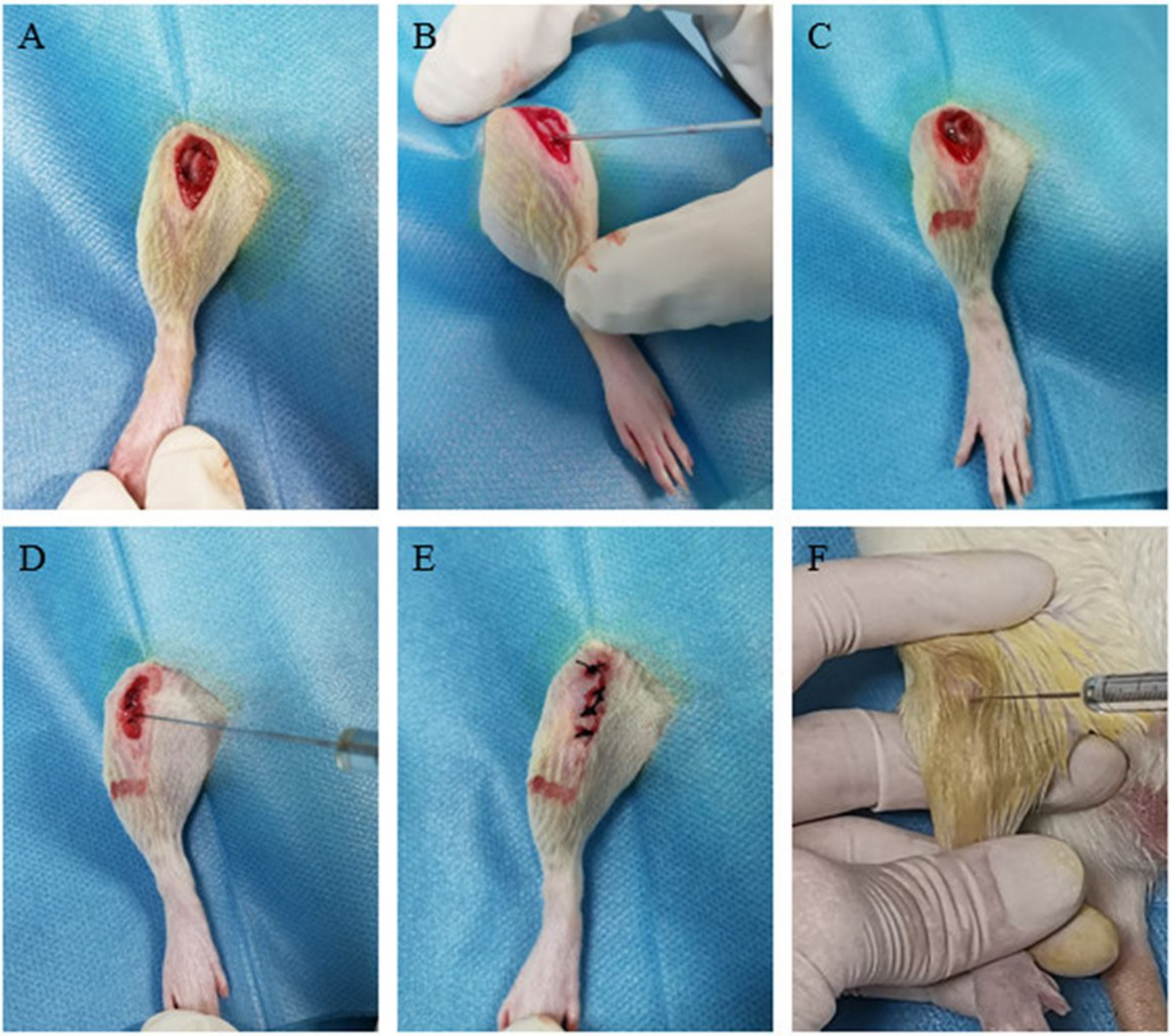

Figure 1

A PJI rat model was established. (A) Medial parapatellar arthrotomy with translocation of the extensor mechanism and exposure of the distal part of the femur. (B,C) The femoral canal is accessed via the intercondylar notch and reamed with sequentially larger needles, followed by retrograde insertion of the K-wire into the femoral canal. (D) Local injection of staphylococcus aureus suspension into the joint space after joint capsule closure. (E) Skin closure with interrupted 4# sutures. (F) Injection of D-AAs into the joint by microsyringe at regular intervals.

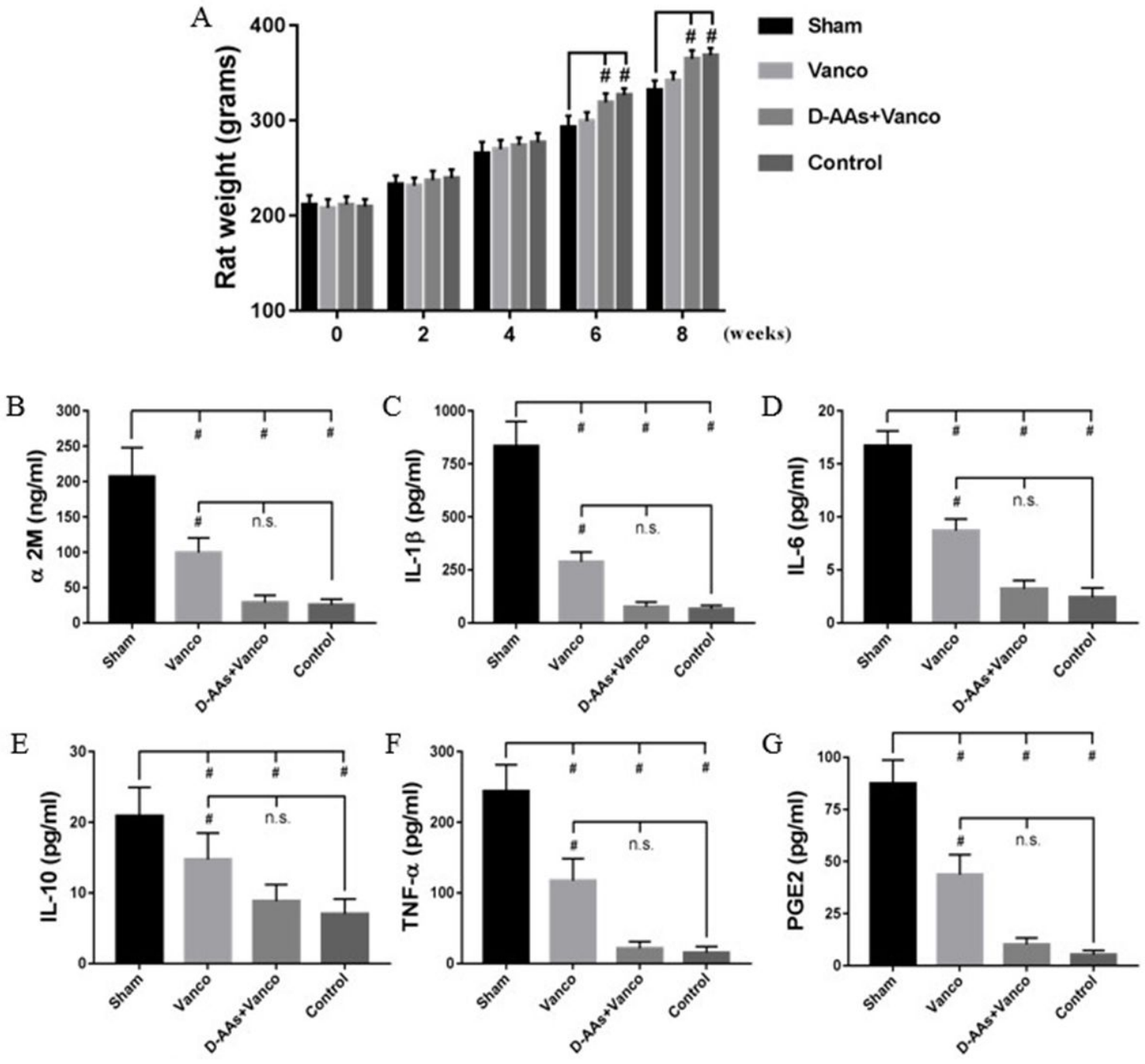

Figure 2

Bar graphs of weight and serum markers. (A) The changes in rat weight over time. n = 8 per group. #p < 0.01. (B) The levels of α2M, IL-1β, IL-6, IL-10, TNF-α and PGE2 in the serum at postoperative 8 weeks. n = 8 per group. #p < 0.01; n.s. (not significant).

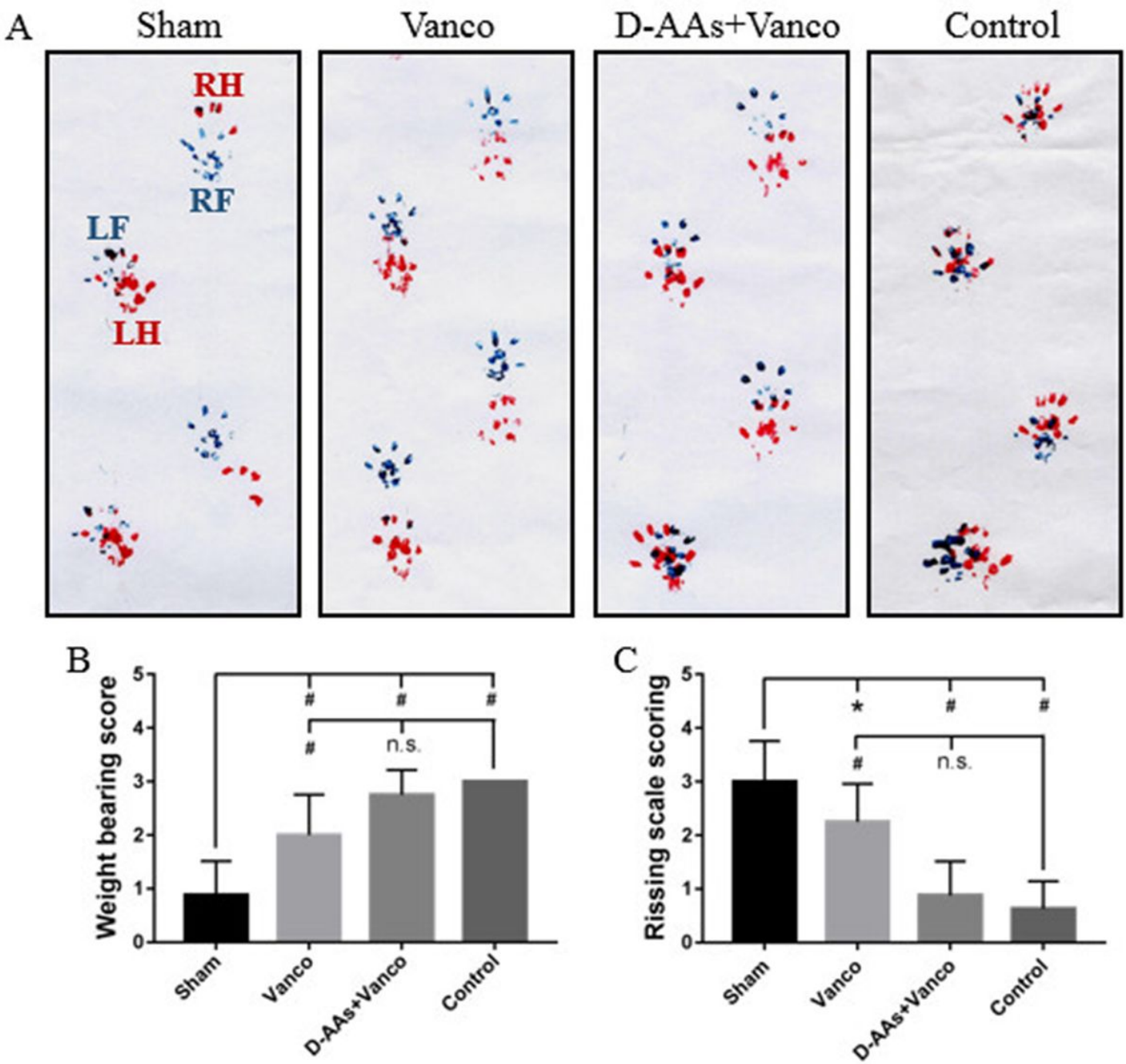

Figure 3

The evaluation of weight-bearing activity and Rissing scale scoring. (A) Representative images of ink blotting trail of different groups. RH, right hind (red); LH, left hind (red); RF, right front (dark blue); LF, left front (dark blue). (B) The grade of weight-bearing activity among the different groups. (C) Rissing scale scoring used for assessment of soft-tissue and bone damage. n = 8 per group. *p < 0.05; #p < 0.01; n.s. (not significant).

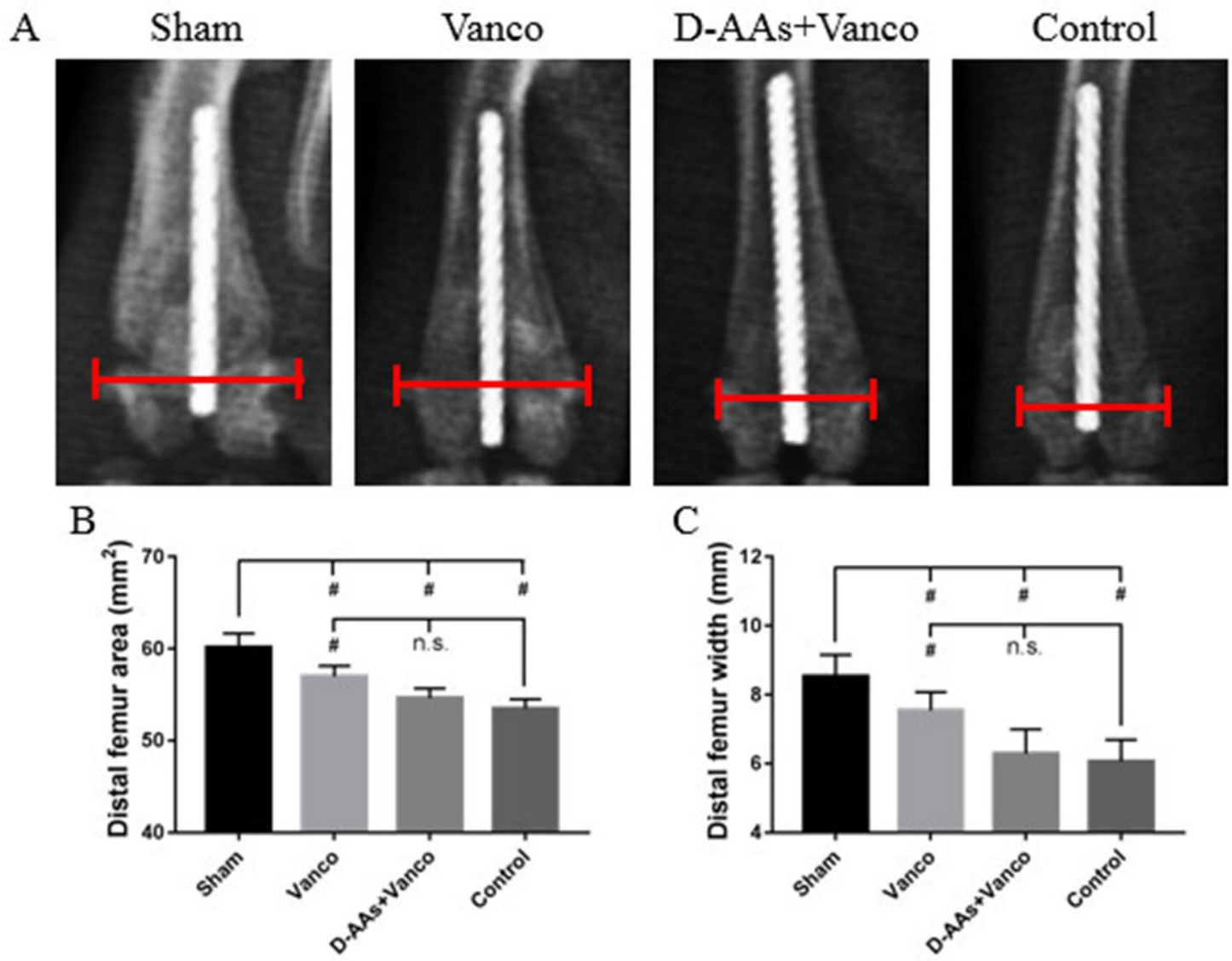

Figure 4

The bone changes observed on X-ray images. (A) Representative anteroposterior (AP) X-ray images demonstrating distal femur bone changes of controls as well as staphylococcus aureus-infected rats treated with sham injection, vancomycin alone, or vancomycin plus D-AAs. (B,C) Quantitative analysis of areas and widthes of distal femur at postoperative 8 weeks. n = 8 per group. *p < 0.05; #p < 0.01; n.s. (not significant).

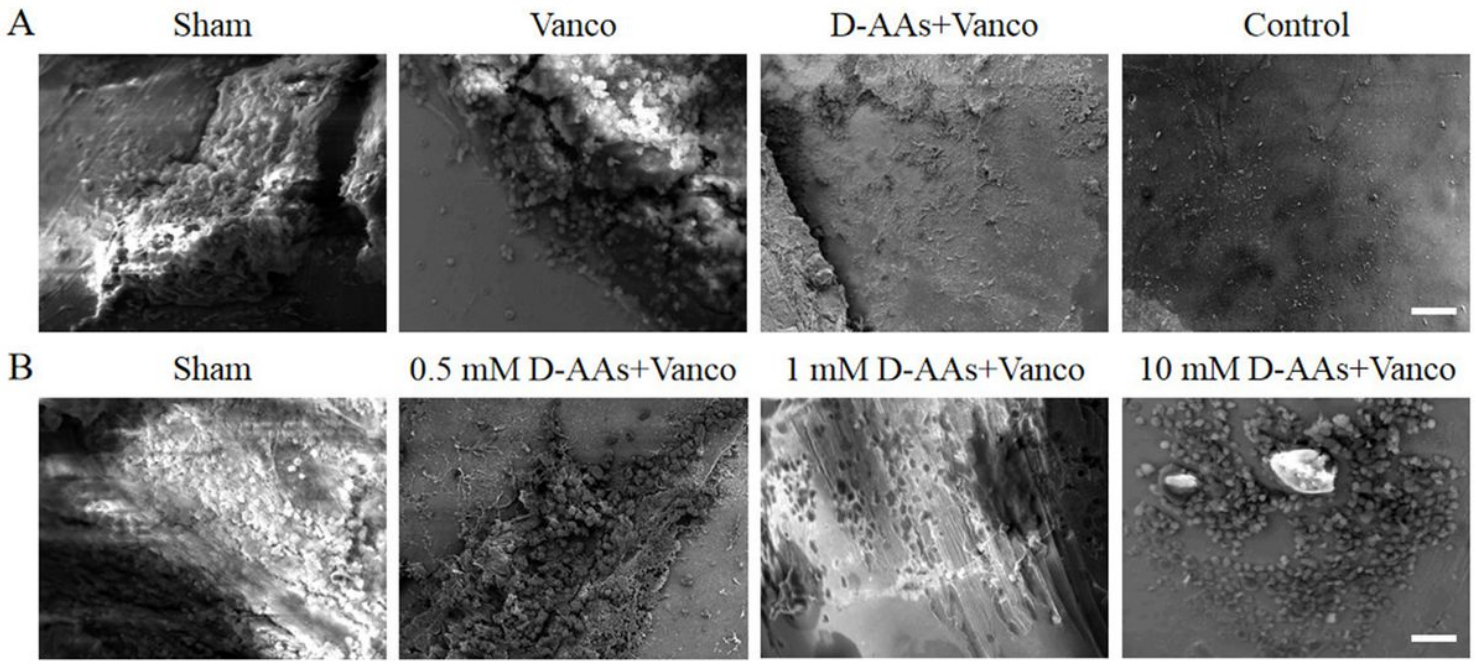

Figure 5

The effect of D-AAs treatment on biofilm formation assessed by scanning electron microscope (SEM). (A-D) Representative SEM images demonstrating biofilm formation on the implant of PJI rats and staphylococcus aureus-infected rats treated with vancomycin alone or vancomycin plus D-AAs as well as controls. Scale bar, 500 μm. n = 4 per group. (E-F) Representative SEM images demonstrating biofilm formation of staphylococcus aureus-infected rats treated with sham injection or D-AAs at multiple concentrations. Scale bar, 500 μm. n = 4 per group.

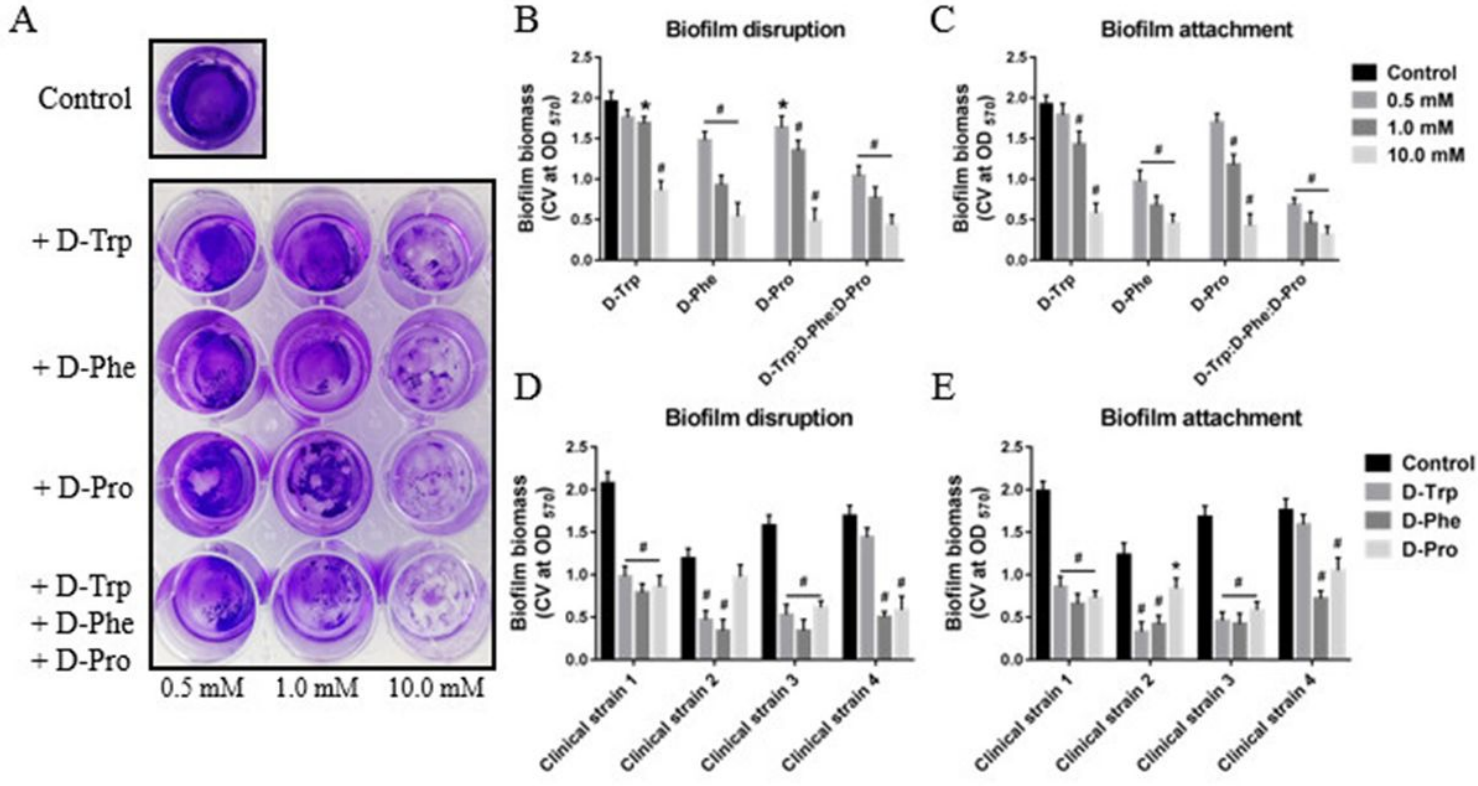

Figure 6

The Dispersion and inhibition of biofilm by D-AAs in different staphylococcus aureus strains. (A) Representative images of CV-stained biofilms from staphylococcus aureus ATCC25923 following overnight treatment with individual D-AAs. (B,D) Dispersion of formed biofilm: Biofilm biomass (OD570) following treatment of formed biofilms of staphylococcus aureus ATCC25923 and four representative clinical isolates of staphylococcus aureus with each individual D-AA (tryptophan (Trp), phenylalanine (Phe), proline (Pro)) or an equimolar mixture of D-AAs. (C,E) Prevention of biofilm formation: Biofilm biomass for the staphylococcus aureus ATCC25923 and same clinical isolates following co-incubation of the bacteria with each individual D-AA or an equimolar mixture of D-AAs. Data are presented as the mean ± standard deviation of three independent experiments. *p < 0.05.

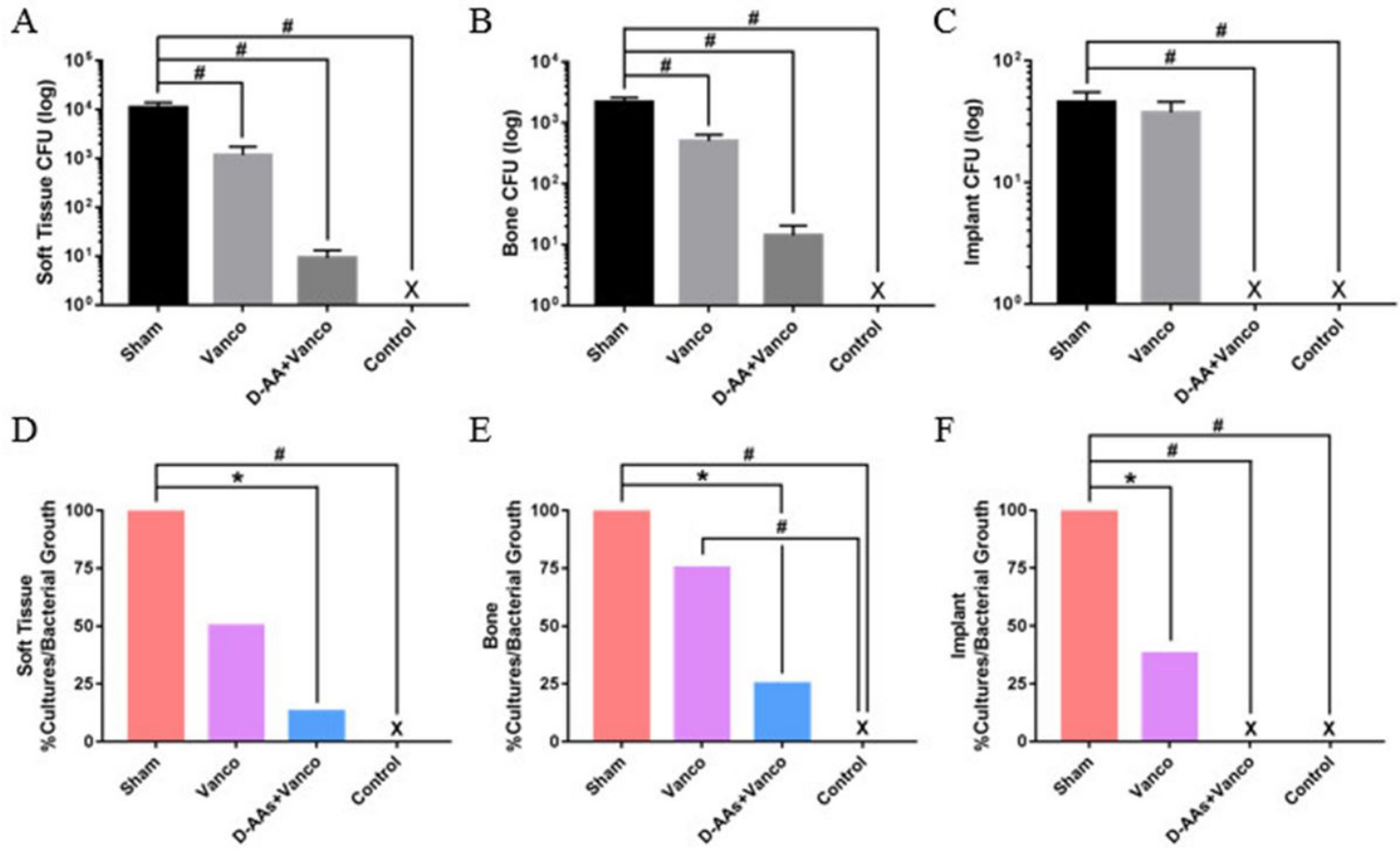

Figure 7

The quantity of bacteria burden in the soft tissue, bone, and implant at 6 weeks after interventions. (A-C) The numbers of bacteria isolated from the soft tissue, bone and implants. (D-F) The percentages of cultures showing positive bacterial growth for each specimen type. n = 8 per group. X, a value of 0. *p < 0.05. #p < 0.01.

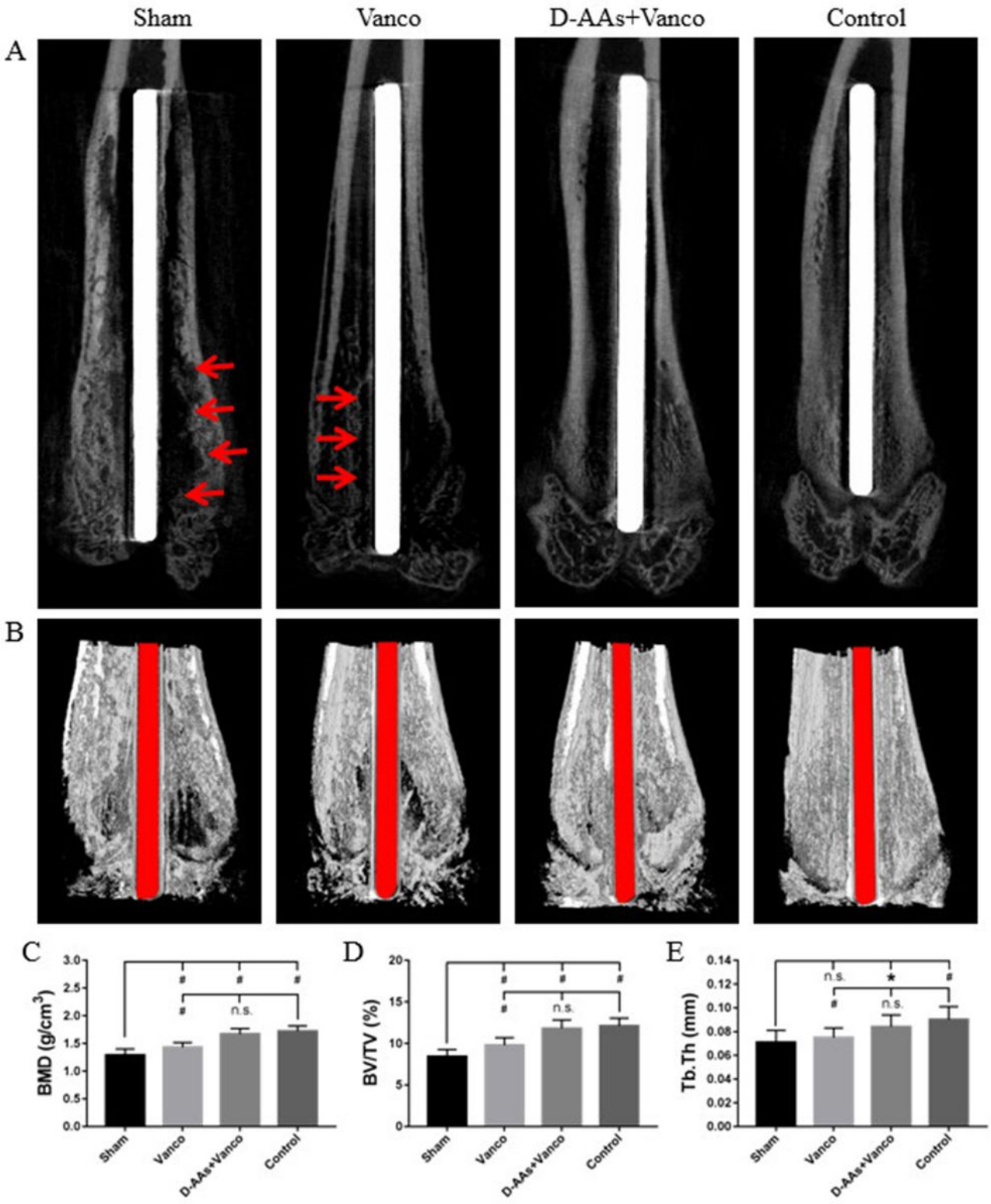

Figure 8

The changes of bone microstructure around the implant at 6 weeks after treatment. (A,B) μCT images of coronal views of distal femur. Red arrow marked osteolysis. (B-D) Quantitative μCT analysis of distal femur of bone mineralization density (BMD), bone volume fraction (BV/TV), and trabecular thickness (Tb.Th). *p < 0.05; #p < 0.01; n.s. (not significant).

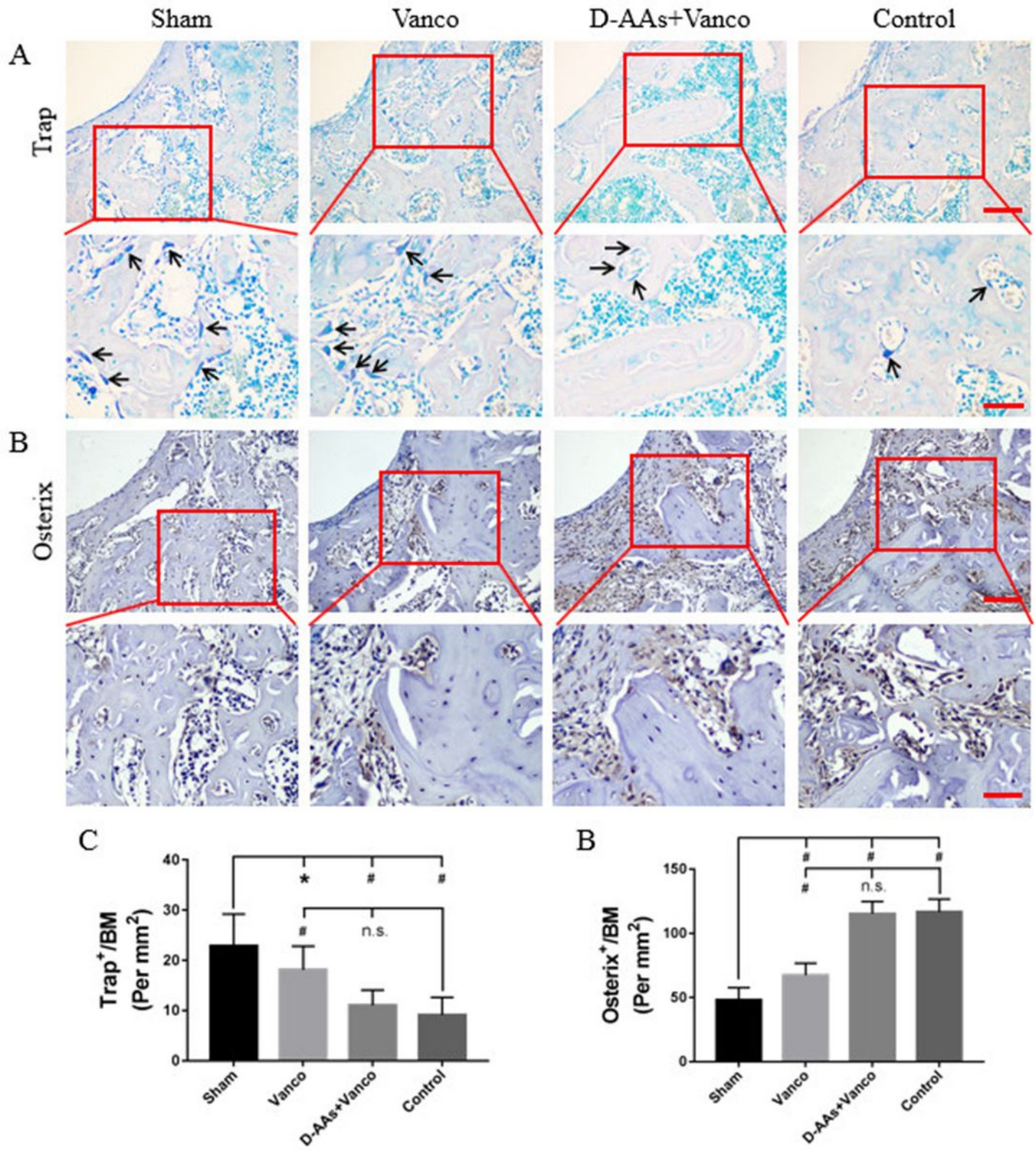

Figure 9

The aberrant bone remodeling around the implant defined by immunostaining for markers of different bone cells at 6 weeks after treatment. (A) Immunostaining and quantitative analysis of tartrate-resistant acid phosphatase (TRAP) at 6 weeks after treatment. Scale bar, top-100μm, bottom-50μm. (B) Immunohistochemical staining and quantification of osterix+ cells around implant at 6 weeks after treatment. Scale bar, top-100μm, bottom-50μm. *p < 0.05; #p < 0.01; n.s. (not significant).

Supplementary Files

This is a list of supplementary files associated with this preprint. Click to download.

- SupplymentaryFigure1.jpg
- SupplymentaryTable1.xlsx